Mohan Kumar et al. 2018. *Int. J. Vehicle Structures & Systems*, 10(5), 324-328
ISSN: 0975-3060 (Print), 0975-3540 (Online)
doi: 10.4273/ijvss.10.5.03

International Journal of Vehicle Structures & Systems
Available online at www.maftree.org/eja

Numerical Investigation of Pressure Drop for Various Models of Catalytic Converter to Capture CO_2 Emission using Activated Carbon

S. Mohan Kumar[a] and S. Satish[b]

Dept. of Automobile Engg., Kumaraguru College of Tech., Coimbatore, India
[a]*Corresponding Author, Email: mohankumars.auto@kct.ac.in*
[b]*Email: satish.s.auto@kct.ac.in*

ABSTRACT:

Internal combustion engines are found to be extensively used in both mobile and stationary applications. The major drawbacks in diesel engines are the release of harmful gases like HC, CO, NO_x and PM into atmosphere. There is several pre combustion and post combustion techniques are available to control these emissions effectively. Although CO_2 emissions from I.C engines considered as a regulated emission but it is a leading contributor towards Greenhouse gases. In this work a numerical investigation on backpressure was carried out by varying porosity factor of activated carbon. Activated Carbon seems to be viable substance to capture CO2 emission from diesel exhaust. To evaluate the backpressure an analysis was carried out using CFD ANSYS fluent software. In the present investigation an analysis is carried out by placing activated carbon at three different variations. Then the analysis are done by varying three different porosity percentages 30,35 and 45 by placing activated carbon at three different locations. Final study reveals that activated carbon placed at PC35-3 layout shows optimum backpressure and high filtration efficiency while compared with other two layouts.

KEYWORDS:

Carbon dioxide; Backpressure; CFD ANSYS; Filtration efficiency

CITATION:

S. Mohan Kumar and S. Satish. 2018. Numerical Investigation of Pressure Drop for Various Models of Catalytic Converter to Capture CO_2 Emission using Activated Carbon, *Int. J. Vehicle Structures & Systems,* 10(5), 324-328. doi:10.4273/ijvss.10.5.03.

ACRONYMS AND NOMENCLATURE:

V_v	Porous Void Volume (mm^3)
V_t	Total Volume (mm^3)
d	chamber diameter(mm)
h	chamber height (mm)

1. Introduction

Due to rapid increase in number of automotive industries in the world, resulted increase in exhaust emissions to the environment. Vehicular emissions such as particulate matter, hydro carbon, carbon dioxides, carbon monoxides and nitrogen oxides are hugely responsible for the air quality deterioration [1]. This emission affects both the human beings and the environment to a greater extent. Automobiles are the second largest source for increasing Carbon dioxide (CO_2) gas emission in the atmosphere.CO_2 from internal combustion (IC) engines is a desired product which is said to be formed due to the complete combustion of fuel. However CO_2 is also said to be the major source of Greenhouse gas (GHG) emissions (about 82%).Transportation sector constitutes about 14 % of the total CO_2 emissions [1]. It is necessary to take preventive step to control greenhouse gas emissions from the vehicles. Carbon capture and sequestration (CCS) is the viable technique to control industrial CO_2 emission, whereas in automobiles, there is no after treatment devices to control CO_2 emission.

Absorption, cryogenic distillation, biological methods, adsorption and membrane-based separation are the currently used technologies for CO_2 separation [2]. In the present work an attempt was made to capture CO_2 by using adsorption technique. Conventional solid adsorbents include activated carbons, silica gel, ion-exchange resins, zeolites, meso-porous silicates, activated alumina, metal oxides, carbon fibres, metal-organic frameworks and other surface-modified porous media. A recent review has comprehensively described the adsorbent materials for CO_2 capture from large anthropogenic point sources [3]. In the present work an activated carbon was used to capture CO_2 emission from automobile. A numerical investigation was carried out to evaluate backpressure by placing volumes. Usually IC engines needs some amount of energy for expelling of burnt gases out and admittance of fresh air fuel mixture. During this process gases are pumped from low inlet pressure to higher exhaust pressure this will leads to loss in power.

During the exhaust stroke the piston moves from BDC to TDC to send out the burned gases out. The power required to expel the exhaust gases out is termed as exhaust stroke loss and it increases linearly with engine speed. The network output per cycle is depends majorly on the pumping work, which in turn directly proportional to back pressure. In this present work the CFD analysis is carried out to evaluate the backpressure

by placing activated carbon at three different configurations with three porosity value. The back pressure [4]. Another major aspect associated with backpressure issue is filtration efficiency of a converter, which in turn depends upon the porosity of Activated carbon chosen. In case of filtration efficiency activated carbon with high porosity have less backpressure but it has poor filtration efficiency. Another scenario the activated carbon with less porosity has high backpressure and high filtration efficiency. Optimum design of these parameters needs to be carried out in order to meet current emission norms. Other details like design considerations, boundary conditions and fluid properties etc. will be explained elaborately in the upcoming sections.

2. Mathematical model

The back pressure developed due to the presence of porous medium is numerically determined by using CFD tool. The governing equations considered are continuity equation and Navier stroke Eqn. using,

$$\frac{\partial \rho}{\partial t} + \nabla .(\rho \vec{v}) = S_m \frac{\partial \rho}{\partial t} + \nabla .(\rho \vec{v}) = S_m \quad (1)$$

$$\frac{\partial}{\partial x}(\rho \vec{v}) + \nabla .(\rho \vec{v}\vec{v}) = -\nabla p + \nabla .(\bar{\bar{\tau}}) + \rho \vec{g} + \vec{F} \quad (2)$$

$$\frac{\partial}{\partial x}(\rho E) + \nabla .\left(\vec{v}(\rho E + p)\right) = \nabla .\left(k_{eff} \nabla T - \sum_j h_j \vec{J_j} + \left(\bar{\bar{\tau}}_{eff}.\vec{v}\right)\right) + S_h \quad (3)$$

The turbulence effects are included by using standard $k\varepsilon$ turbulence model:

$$\frac{\partial}{\partial x}(\rho k) + \frac{\partial}{\partial x_i}(\rho k u_i) = \frac{\partial}{\partial x_j}\left[\left(\mu + \frac{\mu_t}{\sigma_k}\right)\frac{\partial k}{\partial x_j}\right] + G_k + G_b - \rho\epsilon - Y_m + S_k \quad (4)$$

$$\frac{\partial}{\partial x}(\rho \epsilon) + \frac{\partial}{\partial x_i}(\rho \epsilon u_i) = \frac{\partial}{\partial x_j}\left[\left(\mu + \frac{\mu_t}{\sigma_\epsilon}\right)\frac{\partial \epsilon}{\partial x_j}\right] + C_{1\epsilon}\frac{\epsilon}{k} \times (G_k + C_{3\epsilon}G_b) - C_{2\epsilon}\rho\frac{\epsilon^2}{k} + S_\epsilon \quad (5)$$

The effect of porous medium in the flow equation is undertaken by including the porous momentum source term. It consists of two parts 1) viscous flow term 2) Inertial loss term.

$$S_i = -\left(\frac{\mu}{\alpha}V_i + C_2\frac{1}{2}\rho|V|V_i\right) \quad (6)$$

3. Geometry and design consideration

The amount of activated carbon required for the adsorption of CO_2 is with respect to the stroke volume of the engine considered. In general 1/3rd stoke volume is considered as required volume for filling activated carbon [5]. The engine specification considered is shown in Table 1. The total volume (V_c) of activated carbon required is,

$$V_c = 1/3 \times V = 1/3 \times 440968.34 = 146989 \text{ mm}^3 \quad (7)$$

The pressure drop reading is obtained for three porosity (ε) values of 30%, 35% and 40%. For each porosity, the number of activated carbon filled chambers inside the silencer is taken as 1, 2 and 3 as shown in Fig. 1. The volume calculation for each chamber is given below,

$$\text{Porosity, } \varepsilon = V_v / V_t \quad (8)$$

Where V_v and V_t is porous void volume and total volume. Consider the condition of ε = 0.4 and number of inside chamber is 3, $V_v = V_t - V_p$, Eqn. (8) becomes,

$$0.40 = \frac{V_v}{V_t}, V_t - V_p = 0.4\, V_t, 0.6\, V_t = V_p$$

Since, $V_t = \frac{\pi}{4} \times d^2 \times h$, where d and h are cross-sectional diameter and height of the activated carbon chamber inside the silencer.

$$0.6 \times \left(\frac{\pi}{4} \times d^2 \times h\right) = V_p, h = \frac{V_p \times 4}{0.6 \times \pi \times d^2}$$

Since, $V_p = \frac{146989}{3}$, due to 3 inside chambers. We have

$$V_p = 48996.44\ mm^3, h = \frac{48996.44 \times 4}{0.6 \times \pi \times 100^2},$$

$$h = 10.39\ mm$$

The h value obtained by changing ε and number of chambers as shown in Table 2.

Table 1: Engine specifications

Specification	Symbol	Units
Bore diameter	D	87.5 mm
Stroke length	L	110 mm
RPM	N	1500
Number of cylinder	n	2
Engine volume	V	440968.34 mm^2

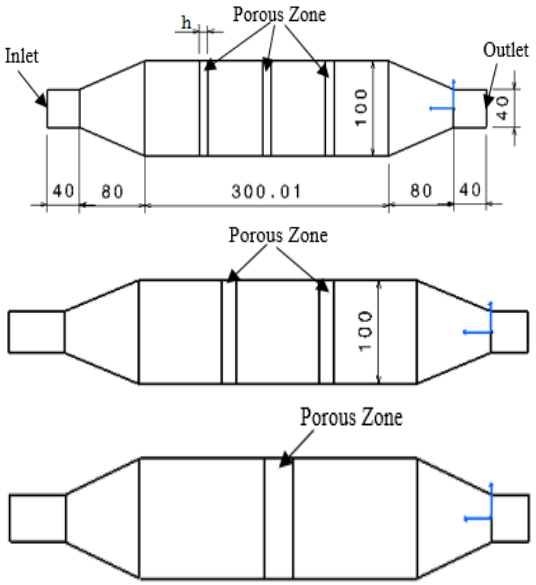

Fig. 1: Silencer draft image for 1, 2 and 3 porous chamber

Table 2: Porosity volume height

Chamber types	Porosity, ε	No of chambers	h (mm)
PC 40-1	0.40	1	31.19
PC 40-2	0.40	2	15.59
PC 40-3	0.40	3	10.39
PC 35-1	0.35	1	28.79
PC 35-2	0.35	2	14.39
PC 35-3	0.35	3	9.59
PC 30-1	0.30	1	26.74
PC 30-2	0.30	2	13.37
PC 30-3	0.30	3	8.91

4. Boundary conditions and meshing

The silencer is connected to the exhaust pipe of the engine, hence velocity of the exhaust coming out of the

engine is considered as inlet boundary condition and atmospheric pressure is considered as outlet pressure since it is open to atmosphere. The exhaust velocity has been measured for the test engine using hot wire anemometer and the maximum velocity reached is 14 m/s at full load condition, hence it is taken as velocity inlet boundary condition. The outlet of the silencer is exposed to atmospheric condition; hence the 0 N/m2 (gauge pressure) is taken as pressure for outlet boundary condition. The packed bed porous medium is considered and it is defined by its direction vector, permeability and inertial losses. The fluid flow properties in the porous region are considered isotropic. The permeability and inertial losses are calculated by the following,

$$\alpha = \frac{D_p^2}{150}\frac{\epsilon^3}{(1-\epsilon)^2} \quad (9)$$

$$C_2 = \frac{3.5}{D_p}\frac{(1-\epsilon)}{\epsilon^3} \quad (10)$$

Where α, C_2, ϵ & Dp are permeability, inertial losses, porosity and diameter of the particle. The diameter of the particle $D_p = 2\ mm$ and porosity is $\epsilon = 0.4, 0.3$ & 0.2 is considered for finding permeability and inertial losses. The obtained α and C_2 for different porosity is given in Table 3.

Table 3: Boundary conditions for CFD

Boundary condition	Values
Velocity Inlet	14 m/s
Pressure outlet (Gauge Pressure)	0 N/m^2
$\frac{1}{\alpha}$ for $\epsilon = 0.40$	2.11 x 10^8 1/m
$\frac{1}{\alpha}$ for $\epsilon = 0.35$	6.8 x 10^8 1/m
$\frac{1}{\alpha}$ for $\epsilon = 0.30$	3.7 x 10^8 1/m
$C_2$for $\epsilon = 0.40$	16406.25 1/m
$C_2$for $\epsilon = 0.35$	45370.37 1/m
$C_2$for $\epsilon = 0.30$	26530.61 1/m

The control volume mesh is created for the element size of 4 mm, 3 mm and 2 mm. Grid independent steady has been done and the results remains unchanged after 2 mm. Hence 2 mm is selected as element size for all the cases. Fig. 2 shows the mesh geometry for PC 40-3.

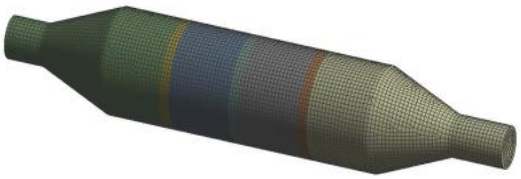

Fig. 2: Mesh geometry for PC 40-3

5. Results and discussions

In the present work as already mentioned the exhaust back pressure is evaluated for three different porosity (0.30, 0.35 &0.40) levels by placing activated carbons at three different positions. The corresponding pressure and velocity plots were shown in Fig. 3 for PC 40-3. The pressure plots for remaining configurations are shown from Figs. 4 to 6. The pressure plot for PC 30-1 is shown in Fig. 4 it shows that pressure drop of around 4.3 kPa is obtained. Compared with other configurations this layout shows maximum pressure drop, this occurs since this layout has higher porosity factor. This scenario restricts the flow of gases it will lead to higher pressure drop across the stream. Similarly the pressure drop of around 4.15 kPa is obtained for PC 30-2 and PC 30-3 configurations and is shown in Figs. 4 and 6. Regarding the filtration efficiency parameters it is high for this layout since it has higher porosity. More active surface layer for physical adsorption of CO_2 is present for this configuration it leads to higher filtration efficiency. On the other hand the higher backpressure produced increases fuel consumption for this layout.

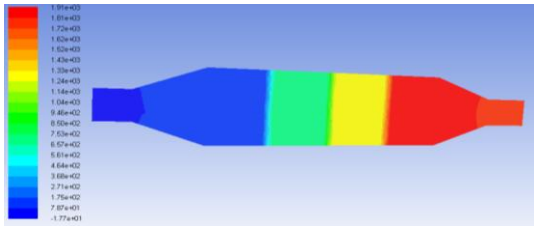

Fig. 3(a): Pressure contour for PC 40-3

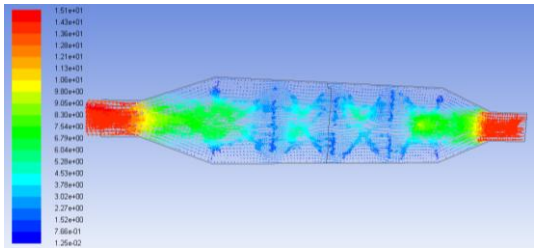

Fig. 3(b): Velocity contour for PC 40-3

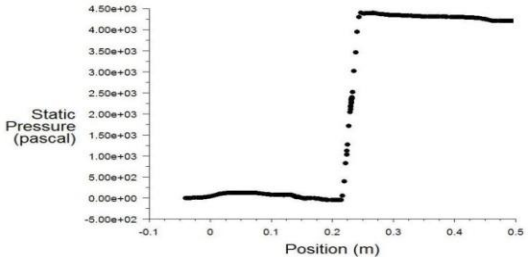

Fig. 4: Pressure plot for PC 30-1

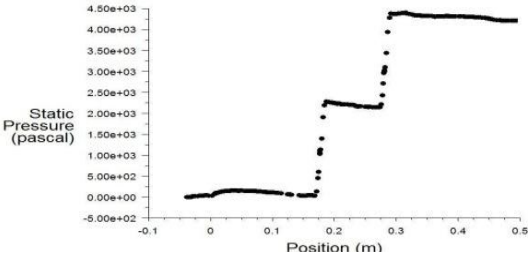

Fig. 5: Pressure plot for PC 30-2

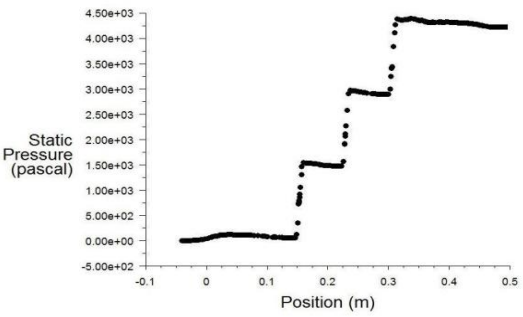

Fig. 6: Pressure plot for PC 30-3

In another study, the pressure plots for PC 35-1, PC 35-2 and PC 35-3 are shown from Figs. 7 to 9. The obtained trend shows that the pressure drop of about 2.75, 2.5 and 2.5 kPa are obtained for PC 35-1, PC 35-2 and PC35-3 layouts respectively. Compared to PC 35-1 the pressure drop for PC 35-2 is higher and it is under acceptable limit. The maximum acceptable pressure drop for the engine setup used in this work is around 3.2 kPa under maximum load condition. PC 35-1 although shows minimum pressure drop while compared with other two layouts it has less reactive surface area this reduces the CO_2 trapping efficiency. The trapping efficiency of CO_2 due to physical adsorption mechanism by Vander walls forces is directly depends upon amount of area utilized for adsorption [6]. The PC 35-2 and PC35-3 almost shows similar pressure drop of around 2.5 kPa, this scenario clearly indicates that pressure drop does not depend upon number of chambers. The pressure drop mainly depends upon the porosity factor it increase linearly with the increase in porosity value. While compared PC 35-2 layout with PC 35-3 the pressure drop is unique but trapping efficiency is higher for PC 35-2 since it has higher surface area for reaction.

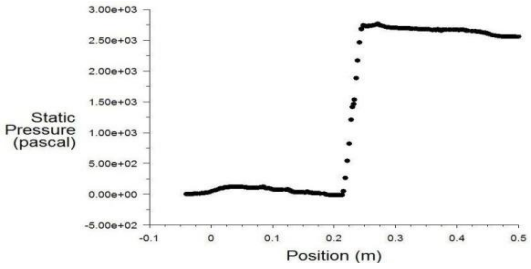

Fig. 7: Pressure Plot for PC 35-1

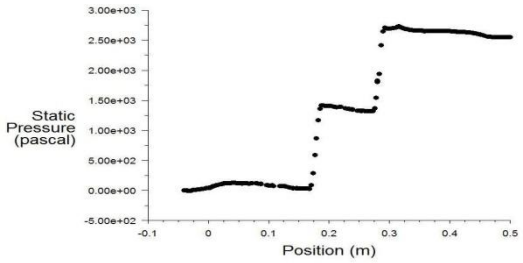

Fig. 8: Pressure Plot for PC 35-2

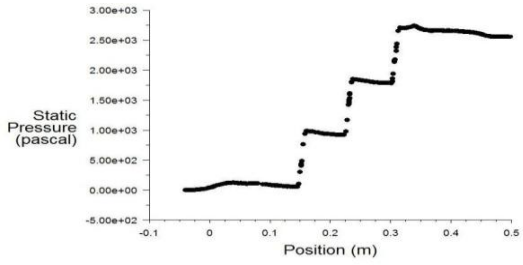

Fig. 9: Pressure plot for PC 35-3

In Final study the pressure plots for PC 40-1, PC 40-2 and PC 40-3 are shown from Figs. 10 to 12. The obtained trend shows that the pressure drop of about 1.8, 1.5 and 1.5 kPa are obtained for PC 40-1, PC 40-2 and PC40-3 layouts respectively. The obtained trend clearly reveals that the pressure drop is very less while compared with PC 30 and PC 35 layouts. Although the backpressure value is much below the acceptable limit this layout has less gas residence time and reaction surface area while compared with other two layouts. Gas residence time is a parameter which determines how efficiently the exhaust gases react on the surface area of an adsorbent. If it increases the trapping efficiency also increases since the exhaust gases has more time to react with the adsorbent. For this layout since it contains more porosity factor the gases easily passes through the porous area and escapes into the atmosphere un-trapped. So this layout PC 40 is practically not feasible to implement for CO_2 adsorption while compared with other two layouts. Considering all the above mentioned reasons the layout PC 35-3 has got many advantages in terms of filtration efficiency and backpressure restrictions. This layout will be further tested by conducting various experiments by various load parameters and results will be summarized.

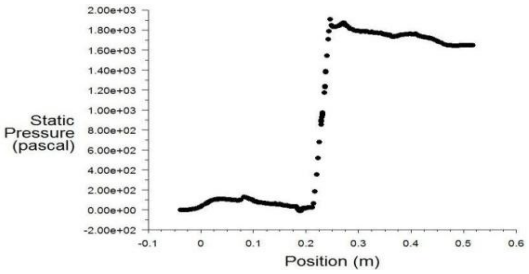

Fig. 10: Pressure Plot for PC 40-1

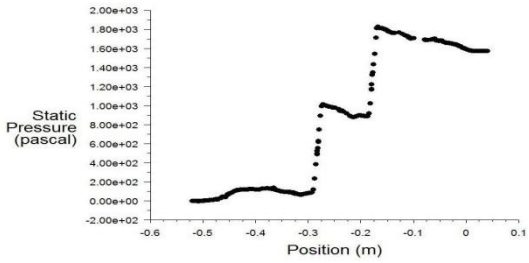

Fig. 11: Pressure Plot for PC 40-2

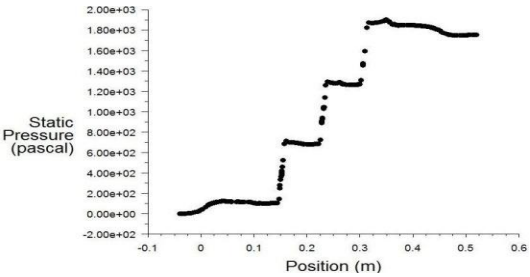

Fig. 12: Pressure plot for PC 40-3

6. Conclusion

In the present work a numerical investigation on various models of catalytic converter is carried out by placing activated carbon at different locations with three different porosity levels. Results obtained shows that a pressure drop of around 4.3 kPa and 4.15 kPa are recorded for PC 30-1, PC30-2 and PC 30-3 respectively. Similarly a pressure drop of around 2.75 and 2.5 kPa is obtained for the layout PC 35-1, PC 35-2and PC 35-3 respectively. Final study for layouts PC 40-1, PC 40-2 and PC 40-3 recorded a pressure drop of around 1.8 and 1.5 kPa respectively. The final conclusion from this study clearly reveals that PC 35-3 shows optimum trapping efficiency and back pressure value while

compared with other two layouts. In further work the same setup is tested in engine under various load conditions and corresponding results will be summarized.

REFERENCES:

[1] A.M. Liaquat, M.A. Kalam, H.H. Masjuki and M.H. Jayed. 2010. Potential emissions reduction in road transport sector using biofuel in developing countries, *Atmospheric Environment*, 44, 3869-3877. https://doi.org/10.1016/j.atmosenv.2010.07.003.

[2] J.R. Li, Y. Ma, M.C. McCarthy, J. Sculley, J. Yu, H.K. Jeong, P.B. Balbuena and H.C. Zhou. 2011. Carbondioxide capture-related gas adsorption and separation in metalorganic frameworks, *Coord. Chem.*, 255, 1791-1823. https://doi.org/10.1016/j.ccr.2011.02.012.

[3] S. Choi, J.H. Drese and C.W. Jones. 2009. Adsorbent materials for carbondioxide capture from large anthropogenic point sources, *Chem. Sus. Chem.*, 2, 796-854. https://doi.org/10.1002/cssc.200900036.

[4] S.M. Kumar and P.S. Kumar. 2015. Numerical and experimental investigation of back pressure in various models of catalytic converter, *Int. J. Applied Engg. Research*, 10(61), 16-23.

[5] S.J. Muthiya, V. Amarnath, P.S. Kumar and S.M. Kumar. 2015. Experimental investigation and controlling of CO_2 emission from automobile exhaust by CCS technique. *Int. J. Applied Engg. Research*, 10(61), 36-46.

[6] C.A. Scholes, S.E. Kentish and G.W. Stevens. 2008. Carbondioxide separation through polymeric membrane systems for flue gas applications, *Recent Patents on Chemical Engg.*, 1, 52-66. https://doi.org/10.2174/2211334710801010052.